Genesis of Hurricane Sandy (2012) simulated with a global mesoscale model

B.-W. Shen,[1,2] M. DeMaria,[3] J.-L. F. Li,[4] and S. Cheung[5]

[1]   In this study, we investigate the formation predictability of Hurricane Sandy (2012) with a global mesoscale model. We first present five track and intensity forecasts of Sandy initialized at 00Z 22–26 October 2012, realistically producing its movement with a northwestward turn prior to its landfall. We then show that three experiments initialized at 00Z 16–18 October captured the genesis of Sandy with a lead time of up to 6 days and simulated reasonable evolution of Sandy's track and intensity in the next 2 day period of 18Z 21–23 October. Results suggest that the extended lead time of formation prediction is achieved by realistic simulations of multiscale processes, including (1) the interaction between an easterly wave and a low-level westerly wind belt (WWB) and (2) the appearance of the upper-level trough at 200 hPa to Sandy's northwest. The low-level WWB and upper-level trough are likely associated with a Madden-Julian Oscillation. **Citation:** Shen, B.-W., M. DeMaria, J.-L. F. Li, and S. Cheung (2013), Genesis of Hurricane Sandy (2012) simulated with a global mesoscale model, *Geophys. Res. Lett.*, *40*, 4944–4950, doi:10.1002/grl.50934.

1.   Introduction

[2]   Storm Sandy (2012) appeared as a low pressure center in the southwestern Caribbean Sea at 18Z 21 October, turned into a tropical depression at 12Z 22 October, and started moving northeastward at 00Z 23 October. It made an unusual northwestward turn at 00Z 29 October and made landfall at 2330Z 29 October near Brigantine, New Jersey, devastating surrounding areas and causing tremendous economic loss and hundreds of fatalities [*Blake et al.*, 2013]. An estimated damage of $50 billion made Sandy the second costliest tropical cyclone (TC) in U.S. history, surpassed only by Hurricane Katrina (2005) [e.g., *Shen et al.*, 2006; *Jin et al.*, 2008, and references therein]. The official track forecasts for Sandy by the National Hurricane Center were good, producing errors that were below the mean official errors for the previous 5 year period, while the model of the European Centre for Medium-Range Weather Forecasts produced remarkable predictions for Sandy [*Kerr*, 2012]. Major scientific debates on this event include the following: to what extent the unique features of Sandy, such as its extraordinarily large scale and its track with a sharp turn during 29–30 October, may be impacted by the current climate; and whether the lead time of severe storm prediction such as Sandy can be extended further [e.g., *Emanuel*, 2012]. In this study, the predictability of Sandy is addressed with a focus on short-term (or extended-range) genesis prediction as the first step toward the goal of understanding the relationship of extreme events such as Sandy with the current climate.

[3]   *Lorenz* [1963a] first classified three kinds of predictability: (1) intrinsic predictability, (2) attainable predictability, and (3) practical predictability, which show dependence on a flow itself, initial conditions (ICs) and mathematical formulas, respectively. In the same year, *Lorenz* [1963b] published another important article that illustrates the sensitive dependence of solutions to ICs, suggesting finite predictability. Since then, numerous studies regarding the chaotic responses that impact weather/climate predictions and hurricane prediction have been published. Among these studies, the chaotic nature of small-scale moist processes has been a focus [e.g., *Zhang and Sippel*, 2009, and references therein]. In comparison, recent observation-based studies [e.g., *Frank and Roundy*, 2006] and modeling simulations [*Shen et al.*, 2010a, 2010b, 2012] were conducted to understand to what extent high intrinsic predictability (of TC genesis) may exist and if and how realistic the corresponding practical predictability can be obtained with advanced global models. Specifically, the role of multiscale processes associated with tropical waves in the predictability of mesoscale TCs has been studied.

[4]   It was reported that the increasing scale of Sandy, in particular during 25–26 October, and its sinuous track with a northwestward turn prior to its landfall are very likely due to the complicated multiscale interactions of Sandy with its environmental flows, such as upper-level troughs and a blocking pattern to the west and east of Sandy, respectively [*Blake et al.*, 2013]. In comparison with Sandy's movement, different multiscale interactions may be involved in Sandy's formation. For example, an easterly wave [*Landsea*, 1993], which originally came from the west coast of Africa on 11 October and moved into the eastern Caribbean Sea on 18 October, was viewed as a precursor of Storm Sandy. During the middle of October, the rising branch of an eastward-moving Madden-Julian Oscillation (MJO) [*Madden and Julian*, 1971] passed by the central Caribbean Sea [e.g., *Blake et al.*, 2013, Figure 1], which could have

---

[1]UMCP/ESSIC, College Park, Maryland, USA.
[2]NASA/GSFC, Greenbelt, Maryland, USA.
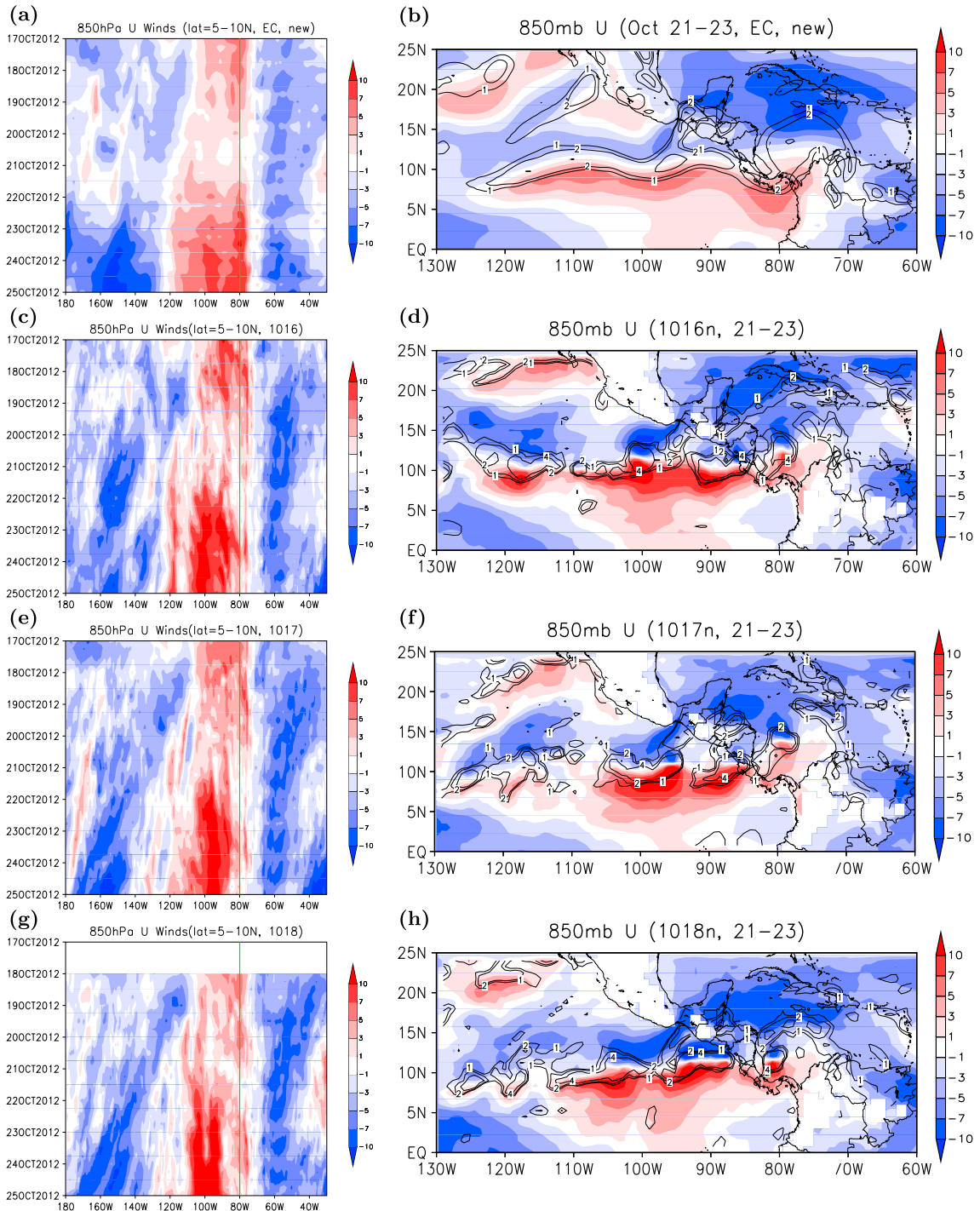[3]NOAA/NESDIS, Fort Collins, Colorado, USA.
[4]CalTech/JPL, Pasadena, California, USA.
[5]NASA/ARC, Moffett Field, California, USA.

Corresponding author: B.-W. Shen, ESSIC, University of Maryland, 5825 University Research Ct. #4001, College Park, MD 20740, USA. (bo-wen.shen-1@nasa.gov)

Figure 1. (a, c, e, and g) Time-longitudinal diagrams of 850 hPa zonal winds averaged over latitudes 5°N to 10°N during the period of 17 to 25 October 2012. (b, d, f, and h) Spatial distributions of 850 hPa zonal winds (shaded, m/s) and vorticity (with selected contour lines of $1 \times$, $2 \times$, $4 \times 10^{-5} \, s^{-1}$), which are averaged over a 2 day period of 00Z 21–23 October. Results for Figures 1a–1h are from the ERA-Interim reanalysis and three model runs initialized at 00Z 16–18 October 2012, respectively.

enhanced convective activity. A low-level westerly wind belt (WWB) that was likely associated with the MJO may have interacted with the easterly wave and thus enhanced cyclonic circulations. During the early stage of Sandy, the appearance of the middle- and upper-level trough over the northwestern Caribbean Sea and Gulf of Mexico (i. e., to the northwest of the Sandy) may have played an important role in Sandy's north-northeastward motion

[*Beven*, 2012; *Blake et al.*, 2013]. From a modeling perspective, the central questions to be addressed are (i) to what extent the multiscale processes, such as the interaction of the eastward- and westward-moving systems and the appearance of an upper-level trough, could impact the timing and location of Sandy's formation and initial movement; and (ii) whether a high-resolution global model can capture these multiscale processes and thus help extend the

lead time of genesis prediction for Sandy. From an alternative perspective, the (potential) intrinsic and practical predictability of Sandy is studied by analyzing global reanalysis data and multiscale simulations from a global mesoscale model (GMM) [e.g., *Shen et al*., 2010a].

[5] The performance of the GMM in simulating TC formations and their associations with different tropical waves was previously examined in a series of papers [*Shen et al*., 2010a, 2010b, 2012]. Selected cases include (i) TC Nargis that formed as a result of the intensification of the northern vortex accompanied with an Equatorial Rossby (ER) wave in late April 2008 in Indian Ocean [e.g., *Shen et al*., 2010a, Figure 3]; (ii) Hurricane Helene that appeared in association with an intensifying African Easterly Wave (AEW) in early September 2006; (iii) Twin TCs that formed through the multiscale processes of a mixed Rossby-gravity wave (MRG) [e.g., *Silva-Dias et al*., 1983] with three atmospheric gyres during an active phase of the MJO in early May 2002. These studies collectively suggest the importance of both large-scale and small-scale processes in contributing to the formation of a TC on the mesoscale [e.g., *Shen et al*., 2012]. The large-scale system (e.g., tropical waves) could provide determinism on the prediction of TC genesis, making it possible to extend the lead time of genesis prediction.

[6] To understand the predictability of hurricane formation, our approach is to examine not only the predictive relationship between a TC and its environmental flows but also the interconnectivity among the environmental flows, which may further help extend the lead time of TC formation prediction. For example, in addition to the association of Hurricane Helene (2006) formation with an intensifying AEW which appeared as the fourth AEW in a 30 day period of 22 August to 21 September 2003, we showed the impact of surface processes on the maintenance of a time-averaged African Easterly Jet which could influence the timing and location in the initiation of multiple AEWs. With regard to the interconnectivity of large-scale flows appearing at the earlier stage of Sandy, *Silva-Dias et al*. [1983] provided insights on the association of the MJO and upper-level trough. The paper is briefly summarized as follows. To explain the appearance of the Bolivian high at 200 hPa and a trough to the east of the high over the Brazil, *Silva-Dias et al*. [1983] proposed a conceptual model by solving the linearized equations of motion on an equatorial beta plane with an imposed heating function, which is asymmetric with respect to the equator. By decomposing the total solution into individual wave modes [e.g., *Silva-Dias et al*., 1983, Figure 4], they related the Bolivian high to the forced Rossby wave and attributed the appearance of the upper-level trough to the eastward dispersion of the MRG and Rossby wave modes at 48 h and 64 h after the release of the heating, correspondingly. We will show that this conceptual model may be applicable to the Sandy case.

[7] In this study, the genesis predictability of Sandy will be studied by performing global mesoscale simulations to (1) illustrate the scale interactions of the WWB and easterly wave and (2) examine the appearance of an upper-level anticyclonic circulation (AC) and trough, their spatial distribution relative to the MJO, and their potential impact on the initial intensification and movement of Sandy. We will briefly introduce the GMM and numerical approaches in section 2 and discuss numerical results in section 3. Concluding remarks are given in section 4.

2. Numerical Approaches

[8] Simulations with the GMM [e.g., *Shen et al*., 2006] are compared with the ERA-Interim T255 (~0.75° or 79 km) reanalysis [e.g., *Dee et al*., 2011] and NOAA National Centers for Environmental Prediction (NCEP) 2.5° reanalysis data. The GMM at the highest resolution of 1/12° (~9 km at the equator) was deployed based on the finite-volume general circulation model [e.g., *Lin*, 2004; *Atlas et al*., 2005].

[9] Control experiments are performed using typical model configurations, including dynamic ICs interpolated from the NCEP analysis, a resolution of 1/4°, large-scale grid condensation scheme with no cumulus parameterizations (CPs). These settings were previously used in our recent TC studies because of their affordability for hurricane climate study. In those studies, we have also presented verifications for the sensitivity of simulations to different dynamic ICs, land surface ICs [*Shen et al*., 2010b] and model physics [e.g., *Shen et al*., 2010a, 2012]. The last one was to understand the uncertainties of different CPs in the simulations of TC genesis. As our main interest is to understand the predictability of Sandy's genesis, we begin with brief discussions on the track and intensity forecasts initialized at 00Z 22–26 October 2012 and focus on the genesis simulation initialized at 00Z 16–18 October 2012. These runs are referred to as "MM/DD," here MM and DD represent the month and day, respectively. For simplicity, genesis in the model is defined as the formation of a low-level closed circulation having a minimum sea-level pressure (MSLP) below 1000 hPa and an elevated warm core in conjunction with a tendency for further intensification [e.g., *Shen et al*., 2010a]. Under these criteria, the genesis timing in each of the three runs is several hours (but less than 24 h) too early. Note that the time difference between a tropical depression and a self-sustaining vortex might be 12–24 h [*Briegel and Frank*, 1997]. To support our conclusion, two tables (Tables S1 and S2) and 10 additional figures (Figures S1–S10) are provided in the supporting information, including wavelength and phase speed analysis of tropical waves and parallel experiments with different CPs.

3. Numerical Results

3.1. Forecasts of Sandy's Track and Intensity

[10] In this section, we discuss the track and intensity forecasts as part of model verifications. Sandy appeared as a low pressure center in the southwestern Caribbean Sea at 18Z 21 October and became a tropical depression with a MSLP of 1002 hPa at 12Z 22 October at (13.1°N, 78.6°W). During the first 2 days, Sandy's movement made a counterclockwise loop within a 2° × 2° domain as shown in the red box in Figure S1a. At 18Z 23 October, Sandy's location was only 50 km away from its initial position at 18Z 21 October. The appearance of the loop is very likely due to the competing impact between the WWB and easterly wave, which will be discussed with the 10/22 and 10/16–18 runs.

[11] Figure S1 displays the five track and intensity forecasts of hurricane Sandy. More detailed error analysis is given in the supporting information. All of runs capture the northwestward turn prior to Sandy's landfall. Three runs (10/23, 10/25, and 10/26) produce accurate and consistent track forecasts. In contrast, the 10/24 run simulates the track with a smooth northwestward turn prior to Sandy's landfall, and the 10/22

run produces larger errors that include an initial error of 151.6 km and an initial clockwise movement, instead of a counterclockwise movement, between 22 and 24 October. The initial erratic track of the 10/22 run may also suggest the impact of the complicated large-scale flows. As our main interest is to study TC genesis, we did not make an attempt at improving the ICs for the vortex (e.g., vortex bogusing). Instead, these experiments are presented to examine the model's performance, in particular in simulating the impact of large-scale flows on TCs at extended-range scales. For example, the 10/23 run produces an accurate track with errors of 127.9, 210.5, and 335.0 km and slightly overestimated intensities with errors of −10.1, −15.5, and −13.3 hPa on Day 6–8, respectively. To illustrate the remarkable predictability on the northwestward turn on Day 6 and landfall on Day 7, the simulated large-scale flows at 500 and 200 hPa levels are compared with NCEP and ERA-Interim reanalysis in Figures S2 and S3, showing good agreement in the simulations of the upper-level troughs and the so-called blocking pattern.

3.2. Simulations of Sandy's Genesis

[12] As discussed earlier, the timing and location of Sandy's genesis and initial movement may depend on the competing impacts of the two environmental flows moving in opposite directions. To illustrate this, we present the ERA-Interim reanalysis and numerical results in Figure 1. Figures 1a, 1c, 1e, and 1g show the time-longitude diagram of 850 hPa zonal winds averaged over latitudes of 5°N to 10°N during the period of 17–25 October. At an earlier time, a WWB occurred between longitudes of 110°W and 75°W (shaded in red in Figure 1a). To the east of the WWB, easterly winds appeared near the eastern Caribbean Sea as the combined flows of the weak preexisting disturbance of the Intertropical Convergence Zone and a westward-moving easterly wave. The ERA-Interim reanalysis shows that the WWB experienced weakening stage between 19 and 21 October, and an intensification after 22 October. Figures 1b, 1d, 1f, and 1h display the spatial distributions of 850 hPa zonal winds (shaded) and vorticity, which are averaged over the 2 day period of 00Z 21–23 October. The ERA-Interim reanalysis (Figure 1b) indicates the appearance of positive vorticity near the interface between the WWB and the easterly winds to its north, which is referred to as the "vorticity zone." Near the leading edge of the WWB where Hurricane Sandy formed, there was a large area of positive vorticity (also shown by the latitude-time diagram of zonal winds in Figures S8d–S8f). Thus, Figures 1a and 1b suggest that the intensification of the WWB and its interaction with the easterly winds may have contributed to the formation of Sandy at 18Z 21 October. Note that in Figure 1a, the westward extension of the WWB is likely associated with the westward energy dispersion of the long wave component of Rossby wave modes generated by equatorial heating near the equator, as suggested by *Silva-Dias et al.* [1983].

[13] Numerical results in Figures 1c–1h suggest that the model with three different ICs can reasonably simulate the intensification of the WWB and spatial distributions of 850 hPa zonal winds. Although the vorticity distribution near the leading edge of the WWB is also captured, the overall spatial pattern of the vorticity zone with local extrema is different from the smooth distribution of vorticity in the ERA-Interim reanalysis. However, due to relatively limited spatial scales and lack of vertical coherence, these vorticity

extrema do not lead to the formation of false-alarm TCs during the target period from the model initial time to 00Z 24 October.

[14] The upper-level 200 hPa winds from ERA-Interim analysis and three model simulations are shown in Figures 2a–2h, respectively. Figures 2a, 2c, 2e, and 2g show the wind vectors and zonal winds (shaded), while Figures 2b, 2d, 2f, and 2h display the meridional winds averaged over a 2 day period of 00Z 21–23 October. In all of the panels, a horizontal (vertical) green line is plotted along latitude 20°N (longitude 80°W) as a reference line. Between latitudes of 5°S and 15°N and longitudes of 100°W and 60°W, there existed an upper-level easterly wind belt (Figure 2a). To the west-northwest and east-southeast of the easterly wind belt, anticyclonic circulations (ACs) appeared in the Northern and Southern Hemispheres. To the east of the northern AC, an upper-level trough can be found, just west of the vertical green line. The overall simulations of ACs and the trough at 00Z 21 October are comparable to the ERA-Interim analysis (in Figures 2a, 2c, 2e, and 2g). By comparison with the study of *Silva-Dias et al.* [1983], the spatial distributions of the northern AC and the trough resemble those in their Figure 6d or 6e, except that their figures need to be flipped over. As discussed earlier, the conceptual model proposed by *Silva-Dias et al.* [1983] suggests that the northern AC is associated with Rossby waves in response to an asymmetric heating, and the trough emerges as a manifestation of the eastward energy dispersion of the short wave components of MRG and Rossby wave modes. Our analysis on the wave dispersion relation with Figure S4 supports this view, showing that the upper-level trough and the northern AC appeared in association with the MRG and ER waves during the active phase of the MJO. The trough in Figure 2 has a slightly larger amplitude and extends farther north than might be expected from an equatorial wave dispersion argument. However, it is possible that an existing trough with midlatitude origins is being amplified by the energy dispersion, especially on its southern end.

[15] The potential impact of the upper-level trough on Sandy's activities is further analyzed with the averaged meridional winds (shaded) in Figure 2b. The horizontal and vertical green lines divide the domain into four quadrants. Near the vertical green line in the second quadrant, the white areas, which represent the transition from the northerly to the southerly winds, roughly indicate the location of the upper-level trough axis. Each of the three experiments produces a 2 day averaged trough with its position slightly shifted to the east of the observed, while the 10/17 and 10/18 runs simulate the troughs with weaker southerly winds between 20°N and 25°N (Figures 2b, 2d, 2f, and 2h).

[16] Figures 3a and 3b show the three forecasts of track and intensity for Sandy after its formation at 18Z 21 October. The overall performance for subsequent track and intensity predictions during the next 2 day period (ending 00Z 24 October) is reasonable, while larger errors occur from 00Z 24 to 25 October (e.g., Figure 3b). For the 10/18 run, its erratic track between 00Z 23 and 24 October appears as a result of the occurrence of two low pressure centers which later merged. As listed in Table S2, the displacement error averaged over the three cases is 271.2 km (315.4 km) on Day 6 (Day 7), while the corresponding RMS errors of MSLP is 4.6 (12.2) hPa. Therefore, it is suggested that the genesis of Sandy can be predicted with a lead time of about 6, 5, and 4 days from the 10/16 to 10/18 runs, respectively.
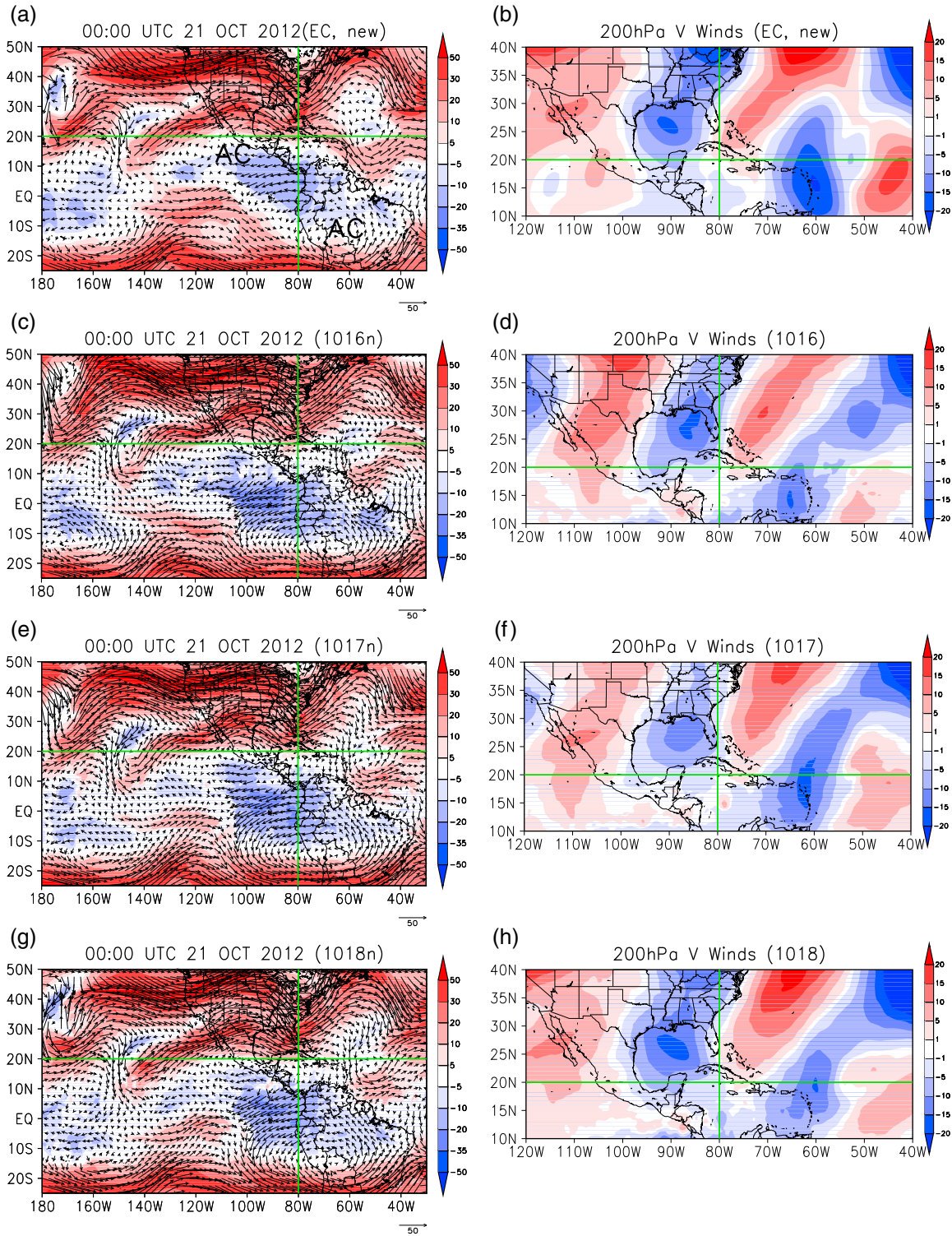
Figure 2. (a, c, e, and g) The 200 hPa wind vectors and zonal winds (shaded, m/s) at 00Z 21 October 2012. (b, d, f, and h) The 200 hPa meridian winds (shaded, m/s) averaged over a 2 day period of 00Z 21 to 23 October. Results for Figures 2a–2h are from the ERA-Interim reanalysis and three model runs initialized at 00Z 16–18 October, respectively. The horizontal (vertical) green reference line is along the latitude of 20°N (the longitude of 80°W). The label "AC" indicates an anticyclonic circulation.

To compare the locations of Sandy's circulation at its initial stage, Figures 3c–3f show the 850 hPa vortex circulation averaged over a 2 day period of 00Z 21–23 October. A location error is measured by the distances between vortex centers from the ERA-Interim and a model run, and the location errors

for the three runs (10/16, 10/17, and 10/18) are 142.6, 247.3, and 256.6 km, correspondingly. In contrast, two earlier runs produce larger location errors of 468.3 km for 10/14 run and 495.6 km for 10/15 run, which are consistent with the less accurate simulation of environmental flows including
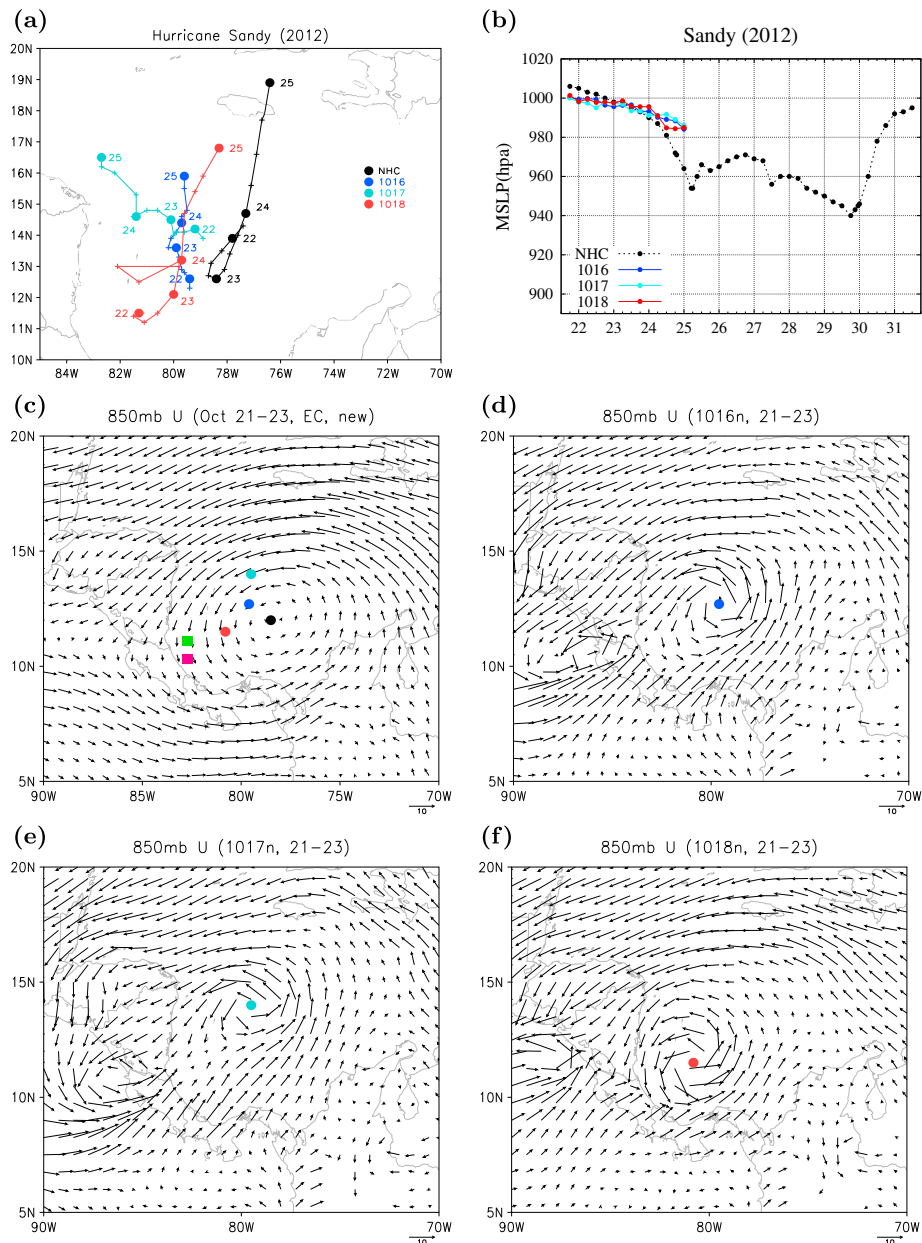
Figure 3. Genesis predictions of Hurricane Sandy in three runs initialized at 00Z 16–18 October, shown in blue, light blue, and red, correspondingly. The black line indicates the best track. (a) The predicted locations of Sandy after its formation. (b) The corresponding minimal sea level pressure from 21Z 21 October to 00Z 25 October. (c–f) The 850 hPa wind vectors averaged over a 2 day period of 00Z 21 to 23 October from EC reanalysis and three model runs, respectively. The vortex centers shown in dots with the same color schemes are at (12°N, 78.5°W), (12.7°N, 79.6°W), (14°N, 79.5°W), and (11.5°N, 80.8°W) in Figures 3c–3f, correspondingly. The closed square in green (pink) indicates the simulated vortex center from the 10/14 (10/15) run.

the WWB in Figure S6a and the upper-level trough in Figure S7d of the supporting information. These two runs are not counted as good genesis forecasts. In addition to the dependence on ICs, the sensitivity of simulations to different moist processes (with CPs), is discussed in Figures S8–S10, indicating the uncertainties of CPs in genesis simulations. This is consistent with our earlier studies [e.g., *Shen et al.*, 2012].

4. Concluding Remarks

[17] In this study, we applied the GMM to investigate the predictability of Hurricane Sandy with a focus on genesis

prediction. We first presented five track and intensity forecasts of Sandy initialized at 00Z 22–26 October, all of which realistically capture its movement with the northwestward turn during the period of 00Z 29–30 October, prior to Sandy's landfall in New Jersey. Among the five experiments, the one initialized at 00Z 22 October produced large errors at the earlier stage of Sandy, which are presumably caused by the combined impacts of a weak initial vortex, model spinning-up processes, and complexity of the environmental flows. The last one, which is indicated by the small loop in Sandy's best track, involved the interactions of the WWB and an easterly wave and could impact the location

and timing of Sandy's genesis. By comparing the runs initialized at 00Z 16–18 October with the ERA-Interim global reanalysis, we demonstrated the model's capability to realistically predict Sandy's genesis with a lead time of up to 6 days (136 h, to be precise) and subsequent evolution for the next 2 day period of 22–24 October. Our study suggested (relatively) high intrinsic and practical predictability for Sandy, as compared to other TCs. The latter can be attributed to the accurate simulations of the following multiscale processes: (1) evolution of the (low-level) WWB associated with the MJO and its interaction with the easterly wave, and (2) the location of an upper-level trough (appearing over the northwestern Caribbean Sea and Gulf of Mexico). The upper-level trough was located in the east of the upper-level AC that appeared in association with the MRG and ER waves during the active phase of the MJO, which deserves to be examined in detail in a future study. The genesis simulations of Sandy provide additional support to the view of the tropical cyclogenesis proposed in *Shen et al.* [2012] which emphasizes (1) the impacts of the large-scale processes (e.g., tropical waves) as well as small-scale processes (e.g., moist processes) in hurricane formation and (2) the importance of large-scale processes in reducing the uncertainties in the location and timing of hurricane formation prediction and thus helping extend the lead time of formation prediction. Due to the imperfection of the model, the (practical) predictability of Sandy in this study may not reach the limit of Sandy's intrinsic predictability. On the other hand, because of the flow dependence for intrinsic predictability, the lead time of Sandy's predictions may not appear in most of the TCs.

[18] Our results showed the dependence of track and genesis prediction on initial conditions. These may suggest the importance in improving the representation of the initial large-scale systems (e.g., tropical waves and trough) and the model's responses to these systems, which include the spinning-up and moist processes.

References

Atlas, R., O. Reale, B.-W. Shen, S.-J. Lin, J.-D. Chern, W. Putman, T. Lee, K.-S. Yeh, M. Bosilovich, and J. Radakovich (2005), Hurricane forecasting with the high-resolution NASA finite volume general circulation model, *Geophys. Res. Lett.*, *32*, L03801, doi:10.1029/2004GL021513.

Beven, J. (2012), Tropical Storm Sandy discussion number (report). National Hurricane Center. Retrieved 2012-10-24.

Blake, E. S., et al. (2013), Tropical cyclone report: Hurricane Sandy, Rep. AL182012. Natl. Hurricane Cent., Miami, Fla.

Briegel, L. M., and W. M. Frank (1997), Large-scale influences on tropical cyclogenesis in the western North Pacific, *J. Atmos. Sci.*, *125*, 1397–1413.

Dee, D. P., et al. (2011), The ERA-Interim reanalysis: Configuration and performance of the data assimilation system, *Q.J.R. Meteorol. Soc.*, *137*, 553–597.

Emanuel, K. (2012), Why America has fallen behind the world in storm forecasting, *Wall St. J.*, http://blogs.wsj.com/speakeasy/2012/10/28/why-america-has-fallen-behind-the-world-in-storm-forecasting/.

Frank, W. M., and P. E. Roundy (2006), The role of tropical waves in tropical cyclogenesis, *Mon. Weather Rev.*, *134*, 2397–2417.

Jin, Y., M. S. Peng, and H. Jin (2008), Simulating the formation of Hurricane Katrina (2005), *Geophys. Res. Lett.*, *35*, L11802, doi:10.1029/2008GL033168.

Kerr, R. (2012), One Sandy forecast a bigger winner than others, *Science*, *338*, 736–737.

Landsea, C. W. (1993), A climatology of intense (or major) Atlantic hurricanes, *Mon. Weather Rev.*, *121*, 1703–1713.

Lin, S.-J. (2004), A vertically Lagrangian finite-volume dynamical core for global models, *Mon. Weather Rev.*, *132*, 2293–2307.

Lorenz, E. (1963a), The predictability of hydrodynamic flow. Transactions of The New York Academy of Sciences, *Ser. II*, *25*(4), 409–432.

Lorenz, E. (1963b), Deterministic nonperiodic flow, *J. Atmos. Sci.*, *20*, 130–141.

Madden, R. A., and P. R. Julian (1971), Detection of a 40–50 day oscillation in the zonal wind in the tropical Pacific, *J. Atmos. Sci.*, *28*, 702–708.

Shen, B.-W., et al. (2006), Hurricane forecasts with a global mesoscale-resolving model: Preliminary results with Hurricane Katrina (2005), *Geophys. Res. Lett.*, *33*, L13813, doi:10.1029/2006GL026143.

Shen, B.-W., et al. (2010a), Predicting tropical cyclogenesis with a global mesoscale model: Hierarchical multiscale interactions during the formation of Tropical Cyclone Nargis (2008), *J. Geophys. Res.*, *115*, D14102, doi:10.1029/2009JD013140.

Shen, B.-W., W.-. K. Tao, and M. L. C. Wu (2010b), African easterly waves in 30-day high-resolution global simulations: A case study during the 2006 NAMMA period, *Geophys. Res. Lett.*, *37*, L18803, doi:10.1029/2010GL044355.

Shen, B.-W., W.-K. Tao, Y.-L. Lin, and A. Laing (2012), Genesis of twin tropical cyclones revealed by a global mesoscale model: The role of mixed Rossby gravity wave, *J. Geophys. Res.*, *117*, D13114, doi:10.1029/2012JD018598.

Silva-Dias, P. L., W. H. Schubert, and M. DeMaria (1983), Large-scale response of the tropical atmosphere to transient convection, *J. Atmos. Sci.*, *40*, 2689–2707.

Zhang, F., and J. A. Sippel (2009), Effects of moist convection on hurricane predictability, *J. Atmos. Sci.*, *66*, 1944–1961.